

Synthesizing multi-log grasp poses*

Arvid Fälldin¹, Erik Wallin¹, Tommy Löfstedt², Martin Servin¹

Abstract—Multi-object grasping is a challenging task. It is important for energy and cost-efficient operation of industrial crane manipulators, such as those used to collect tree logs off the forest floor and onto forest machines. In this work, we used synthetic data from physics simulations to explore how data-driven modeling can be used to infer multi-object grasp poses from images. We showed that convolutional neural networks can be trained specifically for synthesizing multi-object grasps. Using RGB-Depth images and instance segmentation masks as input, a U-Net model outputs grasp maps with corresponding grapple orientation and opening width. Given an observation of a pile of logs, the model can be used to synthesize and rate the possible grasp poses and select the most suitable one, with the possibility to respect changing operational constraints such as lift capacity and reach. When tested on previously unseen data, the proposed model found successful grasp poses with an accuracy of 95%.

I. INTRODUCTION

Grasping and picking up objects comes naturally to humans but is challenging for robots. In unstructured and cluttered environments, autonomous robotic grasping requires robust perception, planning, and control. One example of this is the task of log grasping which plays an important part in modern forestry.

In cut-to-length logging, two types of machines work in pairs during the final harvest: harvesters and forwarders. Harvesters fell and cut trees into logs, and leave them distributed over the forest floor for the forwarder to collect and transport to a nearby road. The forwarding task is repetitive and exposes the operator to harmful whole-body vibrations. The machines are large and heavy, partially to protect the operator, which impacts the environment in the form of soil damage and CO₂ emissions. This motivates research that targets automation and teleoperation.

Autonomous forwarders would need the ability to pick up logs of arbitrary sizes from any log pile configuration. To compete with expert human performance, they would also need to grasp multiple logs at a time, an ability requiring deliberate selection of where and how to grasp in a given pile. The problem of inferring suitable grasp poses from images is known as *grasp synthesis*. Since the advent of convolutional neural networks (CNNs), many data-driven methods for solving it have been proposed [1], [2], [3], [4], [5]. However, most studies consider the grasping of small,

everyday objects and only consider single-object grasps [6], [7].

Multi-object grasping poses many challenges compared to the single-object case: Objects can, and must, be considered both targets and obstacles depending on one’s intent. Further, objects that are within reach to be grasped together may still form an unstable or poorly balanced configuration inside the gripper, making unloading more difficult. Lastly, if grasps are inferred from a single image, then two grasps associated with the same point, (x, y) , may be very different in both width and orientation, and the average of valid grasps is not necessarily a valid grasp itself. This can cause problems when treating the synthesis as a regression task [8].

Log grasping can be considered a special case of multi-object grasping where the target objects may vary in size but all share roughly the same shape. Autonomous log grasping has been explored in the past few years; Andersson *et al.* [9] and Wallin *et al.* [10] used reinforcement learning to pick up logs in simulated environments, but both methods rely at least partially on access to an *a priori* target pose for the crane grapple. La Hera *et al.* [11] demonstrated autonomous single-log grasping on a real platform. Ayoub *et al.* [12] showed how the recent progress of instance segmentation models [13], [14], combined with generic grasping datasets, are applicable to grasping individual logs and groups of logs.

However, we argue that models trained for single-object grasping will inevitably be limited in their ability to synthesize multi-object grasps and that models must be trained specifically for multi-object grasping to have a chance of reaching optimal performance. Furthermore, if one merely tries to identify which grasps are possible, then solutions are non-unique, and the number of solutions can easily be on the order of thousands even with a coarse discretization of the solution space. This suggests using additional metrics, other than graspability alone when searching for optimal grasps.

In this work, we explored multi-object grasp synthesis from RGB-Depth (RGB-D) image data using physics simulations and data-driven models. Our main contributions are the following:

- We show how instance segmentation masks can be used to generalize grasp synthesis to multi-object grasps.
- We expand the notion of grasp quality to include metrics beyond the binary quality measure conventionally used, and show how these can impact the choice of grasp during inference.
- A publicly available, synthetic, dataset of rendered images of log piles, annotated with simulated grasp data.

We assumed access to an instance segmentation model. For each combination of target logs, a target mask was

*This work was partially supported by Mistra Digital Forest Grant DIA 2017/14 #6, Cranab AB, and the Wallenberg AI, Autonomous Systems and Software Program (WASP) funded by the Knut and Alice Wallenberg Foundation.

¹Department of Physics, Umeå University, SE-90187, Sweden.

²Department of Computing Science, Umeå University, SE-90187, Sweden.

Martin Servin is corresponding author martin.servin@umu.se

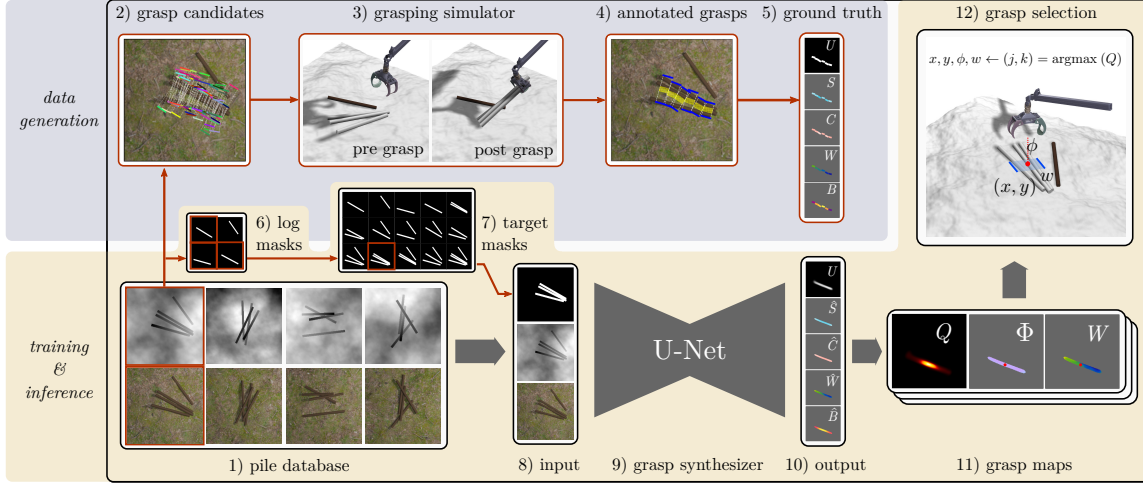


Fig. 1. Model overview. 1) A sample is drawn from the pile database. 2) A rule-based algorithm is used to generate grasp candidates. 3) The grasp candidates are tested in simulation. 4) The pile is annotated with the successful grasps. 5) Grasp annotations are converted into target arrays. 6) Each log in the pile is segmented individually. 7) Individual masks are combined into target masks. With four logs, there are $2^4 - 1 = 15$ possible target subsets to consider. 8) An RGB-Depth image and a target mask are used as input. 9-10) A U-Net model is trained to predict the target variables from Step 5. Steps 2-5 and 8-10 are repeated for each of the 15 target masks. 11) The model output is used to compute the predicted grasp quality in each pixel. We search over all pixels in each of the 15 Q maps and pick the grasp that maximizes the quality. 12) The chosen grasp is tested in simulation.

constructed from the mask of each individual target log. Effectively, the non-target logs were thus treated as obstacles in the cluttered scene. To generate high-quality grasp data we developed a rule-based generator of grasp candidate poses. The candidate grasps were tested in simulation and the successful ones were kept and converted into ground truth grasp maps. The grasp synthesizer’s capability of predicting suitable grasps was tested on previously unseen log piles, including piles of larger size than those used for training. Simulated tests were made using the model to empty a pile of logs through a sequence of grasps and to grasp logs that were tightly packed.

II. METHOD

A. Method overview

The model development was done entirely on synthetic data generated using physics simulation and 3D graphics. We began by generating a collection of artificial log pile samples and for each pile, we rendered an RGB-D image and generated instance segmentation masks for all tree logs. Via multibody dynamics simulations, we were able to find examples of good grasp poses for each pile. Successful grasps were encoded into image arrays to form so-called grasp maps. We then trained a CNN model to predict grasp maps from RGB-D images. Again using simulation, we evaluated the proposed model’s ability to infer high-quality multi-log grasp poses for arbitrary pile configurations. The method is summarized in Fig. 1.

B. Synthesizing grasps

Grasp synthesis is the process of producing grasp tuples, $\tilde{\mathbf{g}} = (\mathbf{r}, \mathbf{p}, w)$, from image data, where $\mathbf{r} = (x, y, z)^\top$ is the grasp position, $\mathbf{p} \in \mathbb{R}^3$ is the gripper pose, and w is the grasp width. If we assume the gripper moves only in

the vertical direction, then the approach orientation can be described with a single angle, ϕ , and the gripper’s vertical position z can be inferred from the depth image given a position, (x, y) . To be able to rank grasps, we also include a grasp quality measure, q , giving us the final grasp tuple definition $\mathbf{g} = (x, y, \phi, w, q)$.

A common approach for synthesizing grasp tuples, introduced by Morrison *et al.* [1], is to learn a function $\mathbf{I} \mapsto \mathbf{G}$, where \mathbf{I} is an image of a scene of objects and $\mathbf{G} = (\Phi, W, Q)$, is a *grasp map*, a three-channel image of the same height and width as the input, that contains the respective grasp parameters, (ϕ, w, q) , in each pixel. Given \mathbf{G} , an optimal grasp, \mathbf{g}^* , can be estimated via

$$(j, k) = \arg \max_{(m, n)} Q_{mn}, \quad (1)$$

$$\mathbf{g}^* = (x(j, k), y(j, k), \Phi_{jk}, W_{jk}, Q_{jk}),$$

where the mapping $(j, k) \mapsto (x, y)$ usually is trivial. Grasps are assumed to be π -periodic with respect to the grasp angle ϕ , *i.e.*, using $\phi = \phi_0 + n\pi$ results in the same grasp for all integers n .

C. Input features and target maps

As input features, we used a five-channel image $\mathbf{I} = (R, G, B, D, M_T)$, *i.e.*, an RGB-D image, together with what we call a target mask, M_T . The RGB-D image contains a top-down view of the log pile, captured with an orthographic perspective by a virtual camera placed 5 m above the ground. The M_T is defined as the union $M_T = \bigcup_{i \in T} M_i$, where M_i is a binary mask indicating all pixels that are part of the i th log. The T is a set that contains the indices of the logs we consider as targets. Instead of letting the model output all valid grasps at once, we trained it to output valid grasps conditioned on that we want to pick up logs marked by M_T .

This conditioning allowed the model to associate multiple different grasps with the same pixel if needed. Using the union M_T as input rather than the individual masks M_i lets us target an arbitrary number of logs while keeping the size of the input fixed. Note that the model was not given access to the mask of non-target logs, which forced it to use the RGB-D input to learn how to avoid obstructing logs in the scene.

As target variables, we used a five-channel image, $G = (C, S, W, U, B)$. The C and S encodes the grasp angle, ϕ , as $C_{jk} = \cos(2\Phi_{jk})$ and $S_{jk} = \sin(2\Phi_{jk})$, respectively. This is the same component-wise encoding as the one used by Morrison *et al.* [1], and makes it easier for a neural network to learn the π -periodicity of the grapple orientation [15]. The W encodes the grasp width w in each pixel, and ranges from 0.30 m to 1.55 m. The U is an indicator image, with pixels close to a successful grasp labeled 1 and others 0. While perfectly binary in the ground truth data, it can take on any value in $(0, 1)$ in the model output. To emphasize the difference, we will refer to this value as the *graspability* when talking about the model’s continuous output.

To be able to separate the good grasps from the ones that are merely possible, we introduce a *balance map*, B . The balance map encodes the grapple balance value, which is defined as the cosine of the angle β that the grapple makes with the world z -axis after a completed grasp. Definitions of the grapple angle, width, and balance are illustrated in Fig. 2.

The indicator image U is what is commonly denoted as the quality map Q in grasp synthesis. However, in multi-object scenes, the number of valid grasps is typically large, and we argue that a binary metric is insufficient when forming more sophisticated grasp plans. Therefore, we extended the notion of grasp quality to include other metrics via a quality function f acting element-wise:

$$Q_{jk} = f(U_{jk}, \tau, B_{jk}), \quad (2)$$

where τ is the number of target logs — which is the same as the number of logs included in the target mask. Recall that during inference, we chose the grasp that maximizes Q_{ij} in (1). Hence, we could change our definition of grasp optimality by considering different choices of f . And, since the neural network outputs U and B , rather than Q directly, we were free to change our definition of f without having to retrain the neural network.

We explored three different choices of quality functions, f :

$$f_1(u) = u \quad (3)$$

$$f_2(u, \tau; \mu) = u\tau^\mu \quad (4)$$

$$f_3(u, b, \tau; b_{\text{opt}}, \sigma_b) = u\tau^\mu \exp(-(b - b_{\text{opt}})^2 / \sigma_b^2). \quad (5)$$

The f_1 promotes graspability only. This is equivalent to the conventional definition of grasp quality. The f_2 aims to maximize the expected number of grasped logs, and we found empirically that using $\mu = \frac{1}{4}$ gave a good trade-off between graspability and the number of target logs. Finally, f_3 aims

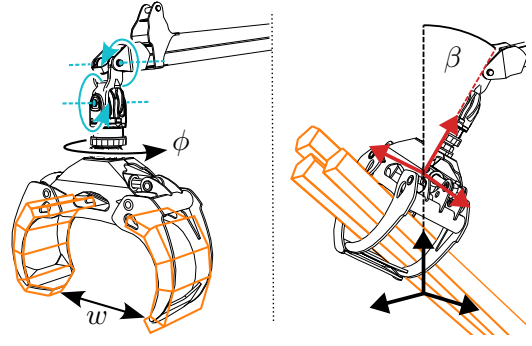


Fig. 2. Definition of the grapple width, w , grapple orientation, ϕ , and balance angle, β . The simplified collision geometry of the grapple and tree logs are shown in orange. Cyan arcs show the rotators’s unactuated joints.

to promote well-balanced grasps with high graspability by weighting the quality by how close the predicted balance value is to optimal balance. The b_{opt} denotes which value we consider to be optimal, and σ_b how harshly we penalize grasps that deviate from b_{opt} . We chose to use $b_{\text{opt}} = 1$ as the optimal balance value and found empirically that $\sigma_b = 0.25$ was a suitable value.

D. Model architecture and training

We estimated the function $\mathbf{I} \mapsto \mathbf{G}$ using a 4.1M parameter UNet [16]. As loss, \mathcal{L} , we used a linear combination of binary cross entropy, \mathcal{L}_{BCE} , and what we refer to as a *masked mean squared error* (MMSE), $\mathcal{L}_{\text{MMSE}}$:

$$\begin{aligned} \mathcal{L}(C, \hat{C}, S, \hat{S}, W, \hat{W}, U, \hat{U}, B, \hat{B}) = \\ \mathcal{L}_{\text{BCE}}(U, \hat{U}) + \lambda_C \mathcal{L}_{\text{MMSE}}(U, C, \hat{C}) + \lambda_S \mathcal{L}_{\text{MMSE}}(U, S, \hat{S}) \\ + \lambda_W \mathcal{L}_W(U, W, \hat{W}) + \lambda_B \mathcal{L}_{\text{MMSE}}(U, B, \hat{B}), \end{aligned}$$

where the λ s are regularization parameters, and hatted variables denote model outputs. The MMSE loss function is defined as

$$\mathcal{L}_{\text{MMSE}}(U, Y, \hat{Y}) = \frac{1}{N^2} \sum_{j=1}^N \sum_{k=1}^N u_{jk} \varepsilon_{jk}^2, \quad (6)$$

where $\varepsilon_{jk} = y_{jk} - \hat{y}_{jk}$ and N denotes the image dimensions (both height and width). For the width map, we used a skewed version of (6),

$$\mathcal{L}_W(U, Y, \hat{Y}) = \frac{1}{N^2} \sum_{j=1}^N \sum_{k=1}^N u_{jk} [(1 - \gamma) \varepsilon_{jk}^2 + \gamma \varepsilon_{jk} |\varepsilon_{jk}|]. \quad (7)$$

By letting $\gamma \in (0, \frac{1}{2})$, we penalize positive errors more than negative ones, with the motivation that grasping too widely is sometimes bad, but grasping too narrowly is *always* bad. Further, by taking the elementwise product with the ground-truth indicator map, U , in (6) and (7), we only penalize predictions made in pixels that we know are valid grasp points. With this loss, we did not have to make any assumptions about which value to assign pixels outside valid grasps, which would have

been a concern with any regular, unmasked, loss function. Note that the neural network will output values for all pixels, but values outside the grasp zone are ignored by the loss. We used $[\lambda_B, \lambda_S, \lambda_C, \lambda_W] = [120, 30, 30, 60]$ and $\gamma = \frac{1}{3}$. The dataset, trained model, and details about the implementation are available at <http://umit.cs.umu.se/grasp-synthesis>.

We trained on 80% of 3116 annotated samples and used the remaining 20% as the validation set. Testing was done on a separate set of 250 unannotated piles. During training, we used random flips and rotations to augment the data.

E. Grasp candidate reduction

It is a challenge in itself to automatically generate consistent training data when the solutions are non-unique — even in a simulated environment. Our approach was to first run a rule-based search for promising grasps to create a list of what we refer to as *grasp candidates*. We then tested those candidates in simulation until we found enough successful grasps.

The initial search for grasp candidates was entirely based on geometry and did not take any dynamics into account. We emphasize that this search algorithm, while helpful during data generation, would not work for grasp synthesis in the wild as it relies on having access to the exact position, pose, and shape of each tree log. Moreover, even with access to perfect information, we were not able to formulate a simple set of rules that guaranteed successful grasps. This led us to simulate thousands of failed grasp trials during data generation.

The number of grasp candidates for a given target subset of logs could range anywhere from zero to a couple of thousands. When the number of candidates was large, the candidates included many grasps that were almost identical, as well as grasps that were needlessly wide or awkwardly oriented. To reduce the candidate list to a few high-quality grasps, we used Algorithm 1 in the simulations.

Algorithm 1 Grasp candidates reduction

Require: A set, G , of candidate grasp tuples

Ensure: A set, S , of successful grasps

```

1:  $S \leftarrow \emptyset$ 
2: while  $G$  is not empty do
3:   Select the narrowest grasp,  $g$  from  $G$ 
4:   Simulate grasp  $g$ 
5:   if Grasp successful then
6:      $S \leftarrow S \cup \{g\}$  ▷ add  $g$  to  $S$ 
7:     Remove grasps from  $G$  that overlap with  $g$ .
8:   end if
9:    $G \leftarrow G \setminus \{g\}$  ▷ remove  $g$  from  $G$ 
10: end while
```

In step 7 of Algorithm 1, we compute the area of the grasp rectangle intersection between g and all remaining candidates. If the overlap exceeds a threshold value (0.04 m^2), the candidate grasp is discarded. Algorithm 1 typically terminated after finding a handful of non-overlapping grasps.

Giving priority to the narrowest grasp candidates has two advantages: The first is that it places the grasp in the middle of the two outermost target logs. The second is that it removes ambiguity in the grapple angle. With a too-wide grasp, there are many different viable grasp orientations, whereas narrow grasps leave little rotational wiggle room. Hence, prioritizing narrow grasps gave us more consistent/less noisy orientation data.

F. Simulator

We generated synthetic data and evaluated the model using multibody dynamics simulations run using the physics engine AGX Dynamics [17]. The simulated environment consisted of a terrain, tree logs, and a crane grapple. The terrain was represented by a $5 \text{ m} \times 5 \text{ m}$ heightfield, procedurally generated using Perlin noise [18]. Logs were modeled as having a cylindrical rendered geometry but a pentagonal prism as collision geometry, see Fig. 2. The pentagonal cross-section provided rolling resistance, which made the log-log interactions less smooth, and presumably less predictable. The logs' lengths, $\ell \sim \mathcal{N}(2.5 \text{ m}, 0.2 \text{ m})$, and diameters, $d \sim \mathcal{N}(0.16 \text{ m}, 0.01 \text{ m})$, were sampled from normal distributions. We modeled the grapple and rotator as a system of nine rigid bodies held together by ten joints. The rotator was attached to a boom which was under kinematic control. The rotator connected the boom and the grapple via three hinge joints, of which only one was actuated. The two unactuated hinge joints made the grapple compliant, meaning it could for example 'fold' if pressed too hard against a log, or bounce off after high-impact collisions. The grapple's design was based on a scaled-down version of a Cranab CR HD grapple [19], and we tuned its closing strength to roughly match that of its real counterpart. As with the logs, we replaced the grapple's collision geometry with a collection of cuboids to make contact computations faster and more stable. The system is illustrated in Fig. 2.

Pile samples were generated by dropping a stack of logs on the ground and letting them settle into a stable configuration. Segmented log masks and RGB-D images were rendered using Blender [20] and stored along with the position, pose, and size of each log.

Once grasp candidates had been generated for each subset of target logs, we performed grasp trials to confirm if they were indeed viable grasps. A trial started with the grapple positioned directly above the grasp point. We lowered the grapple until the number of logs inside of the grapple was equal to the number of target logs, closed the grapple as much as the force limits allowed us to, and raised the grapple until it had returned to its starting height. A trial was classified as failed if the set of logs ending up in the grapple was not the target logs, if the grapple was not sufficiently closed, or if a collision force acting on the grapple at some point exceeded a threshold value. The second condition was enforced as it is generally advised against lifting logs if the grapple claws do not enclose the load completely. The last criterion helps filter out grasps that would be considered

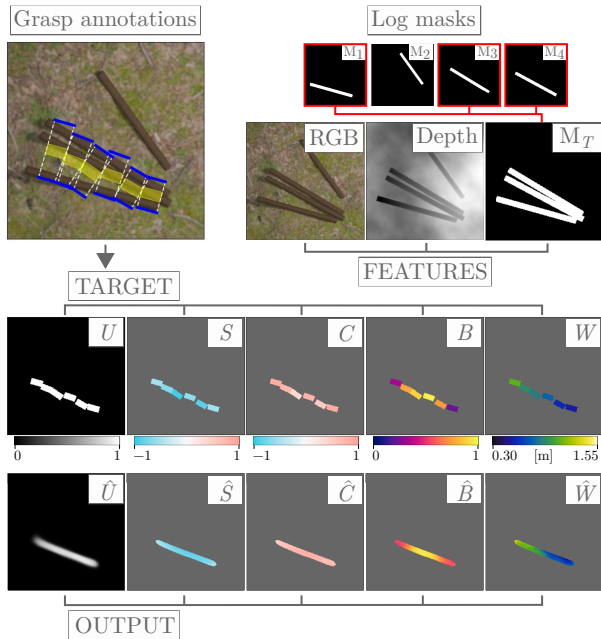


Fig. 3. Illustration of how annotated grasps are encoded into 2D arrays. **Top left:** The thick blue lines show the position of the grapple claw tips, and the yellow areas show the rectangle that we used to encode the grasp parameters in the target arrays. The bottom row shows an example output from the neural network.

reckless and could potentially damage the machine in a real scenario.

Any grasp data we generated would inevitably be biased towards the controller that was used to create them, but we argue that this bias is reduced by using as simple a controller as possible. To further decrease the control dependency, we disabled all contacts between ground and grapple.

G. Synthetic data set

We simulated 212 piles, each consisting of four logs. With four logs, there are $2^4 - 1 = 15$ possible target subsets to consider, and we tried to find valid grasps for each subset. After removing samples that displayed unphysical behavior or unstable log configurations, we were left with 3116 grasp map samples, annotated with 7617 grasps in total. Out of the 3116 samples, 1102 were cases where no successful grasp could be found for the given targets. In addition to these 212 piles, we generated 250 unannotated piles, that we used as the test set.

Each sample consisted of an RGB-D image and a segmented mask of target logs, along with grasp data encoded into 2D arrays as seen in Fig. 3. The encoding was made using the grasp rectangle method proposed by Morrison *et al.* [1]. However, unlike them, we used rectangles of constant width (20 cm) rather than letting the rectangles' sizes be proportional to the grasp width, w . We hypothesized that using proportional rectangle sizes for the indicator channel would lead to a model that assigns higher probabilities to areas surrounding wide grasps.

TABLE I

TEST SET PERFORMANCE IN SIMULATION. β_{AVG} IS THE AVERAGE BALANCE ANGLE, AND β_{MAX} IS THE HIGHEST OBSERVED BALANCE ANGLE. BALANCE STATISTICS ARE CALCULATED USING SUCCESSFUL GRASPS ONLY.

Pile size	Quality function	Success rate	Avg. no. of grasped logs	β_{avg}	β_{max}
4 logs	f_1	97%	3.1	12°	30°
	f_2	95%	3.7	11°	30°
	f_3	99%	3.7	6°	16°
6-7 logs	f_1	79%	3.3	8°	17°
	f_2	73%	3.4	8°	20°
	f_3	78%	3.6	3°	11°

III. RESULTS

A. Overall performance

We tested the proposed model in simulation on the test set of 250 unannotated piles, using three different objective functions to select the optimal grasp in the model output. The performance is summarized in Table I. We found the model to generalize well to new piles of four logs, with a 95%-99% success rate depending on which quality function was used. From Table I we can also see that the quality functions worked as intended, *i.e.*, using f_2 increased the number grasped logs and using f_3 improved the balance of the grasps.

A significant drop in performance was observed when we increased the number of logs to six or seven. After closer inspection of unsuccessful cases, we found that the neural network often outputs too narrow grasps, which led to collisions with the target logs. To confirm that this was indeed the largest source of error, we reran the tests using f_1 , but this time adding 10 cm in grasp width to whichever grasp the model suggested. With this *ad hoc* solution we recovered a success rate of 96%, with 4.2 logs grasped on average. Since the model did not have large issues identifying narrow grasps of five logs or more, our best explanation for this is that the use of only four logs during training has introduced an unintended bias towards closely bundled-up targets.

The root mean squared error in balance angle prediction was 4.2°.

B. Case study — normal pile

To understand how the proposed model is meant to be used, consider the single pile shown in Fig. 4. In each subfigure, we used a unique set of target logs as input to the model. We made one evaluation for each target subset and found the best grasp for each one (here using the quality function f_1). As seen in Fig. 4, the model found sensible grasps for most subsets. We used the model's predicted quality score to rank the different subsets.

C. Emptying a pile with sequential grasps

To illustrate a use case, we applied the model sequentially to empty piles of seven logs with consecutive grasps. One

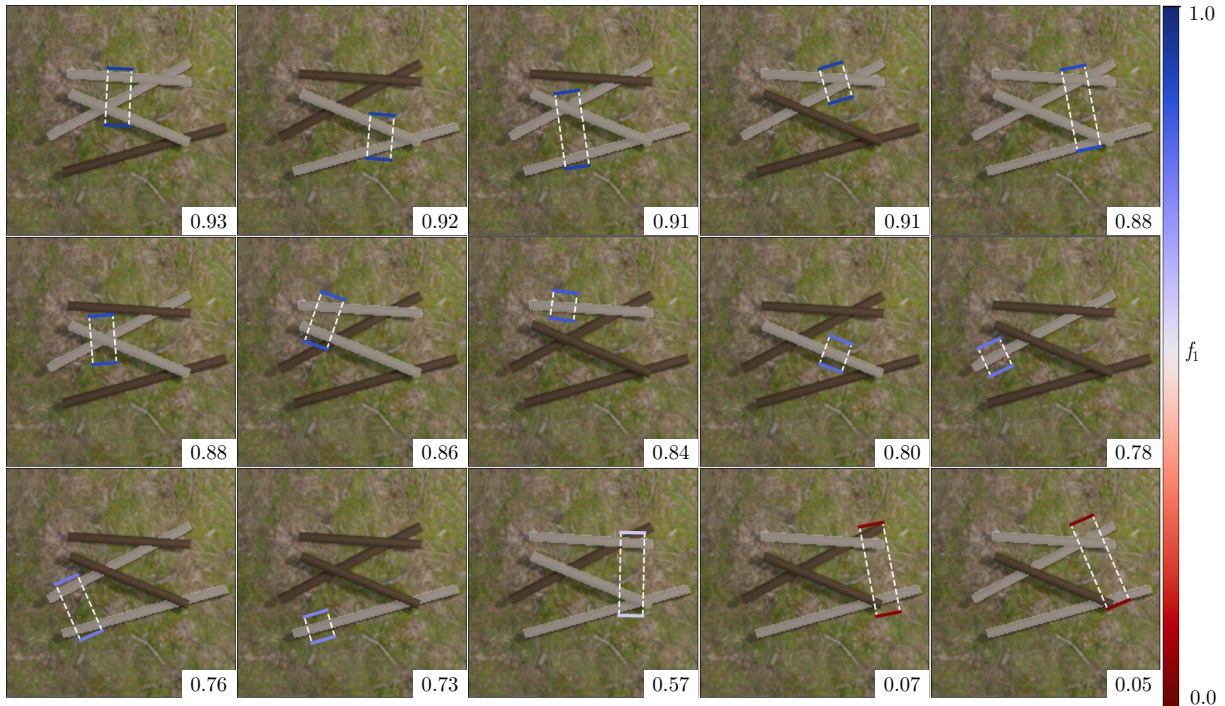


Fig. 4. Optimal grasp for each target subset in a pile. Target logs have been colored white for illustrative purposes. The subsets are ranked from best to worst, and the grasps are color-coded by their graspability score, f_1 , which is also displayed in the bottom right of each subfigure. (Images have been zoomed in by 33% for clarity)



Fig. 5. The model applied in sequence to empty a pile of logs (target masks are not shown in the figures).

such example is shown in Fig. 5. We repeated this process on ten piles and the model was typically able to empty the pile in 2–3 grasps, given that the first grasp was successful. Note that the model lacked the ability to make long-term grasp plans, and would sometimes make grasps that were good short-term but resulted in the remaining logs being spread out too far apart to be grasped together. Also worth noting is that the model tended to target four or more logs in the first grasp, even when we used quality function f_1 , *i.e.* maximizing graspability and not the number of targets. This could be because, for each additional log that was included in the target set, the number of obstacles was also decreased. Hence, a four-log grasp in the training set was also a grasp without any surrounding obstacles.

D. Case study — packed logs

In practice, logs are typically not dropped randomly as in our pile generation process. Instead, they are often found more aligned and tightly packed. It was therefore of interest

to see how the proposed model would do in such scenarios. As shown in Fig. 6, we found the model (here limited to a maximum of four target logs) to consistently output grasps that were correctly aligned with reasonable widths. However, the model showed no tendency to prefer working its way through the pile from outside in, which seemed like the most intuitive strategy. Instead, it assigned more or less the same quality to grasps targeting the pile interior, as shown in Fig. 6d.

E. Perturbation tests

As the proposed method assumes access to segmented masks of each target log, it was motivated to investigate how the model would respond to errors in the target mask. We therefore evaluated the model using incomplete masks, as seen in Fig. 6a-c. We found the model to be robust to the introduced errors, and it typically output grasps such as the ones shown in Fig. 6a-b, whereas erroneous output, such as the colliding grasp shown in Fig. 6c, were rare. We also tested how well the model generalizes to larger logs, by evaluating it on logs twice as thick as the training set average. Again, the model appeared robust to this perturbation, and output reasonable grasps, see Fig. 6e. The perturbation did however affect the graspability score, especially for the two-log grasp in Fig. 6e.

IV. CONCLUSIONS

We conclude that generative grasp models can be trained specifically for multi-object grasping, and that instance segmentation masks can be used to remove the target/obstacle

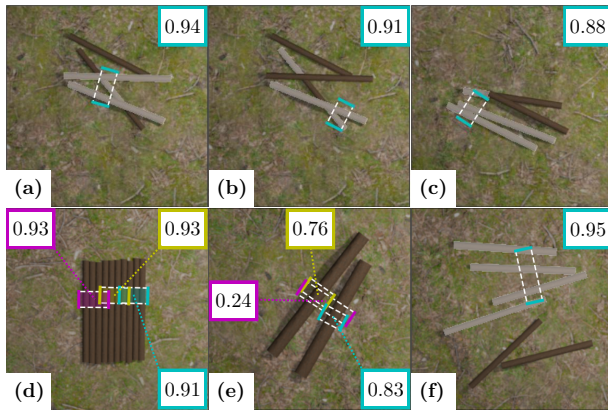


Fig. 6. Example output from the perturbation tests. (a)-(c): Incomplete target mask test. (d) Packed pile test. (e) Size perturbation test, and (f): Example of a model output that resulted in a failed grasp. All shown grasps were selected using the quality function f_1 , and the graspability score is displayed for each grasp.

ambiguity in cluttered scenes. Additionally, the use of segmentation masks allows us to act with intent, making the model outputs easier to interpret. Instance segmentation of tree logs is not an easy task, and this study does in a sense represent performance under ideal conditions. However, the proposed method does not rely on all logs being successfully segmented, only the ones we intend to grasp.

While the proposed method does not replace the need for intelligent control, we believe it has the potential to boost the performance of control solutions that rely on access to grasp poses, such as the one proposed by Wallin et al. [10].

The main limitation of the proposed method is perhaps that the number of possible target subsets increases exponentially with the total number of logs in a pile. Evaluating all possible target subsets would inevitably be computationally limiting as piles grow large. In cases where an exhaustive search over all subsets is not feasible, one could imagine having some pre-processing step where only the most relevant subsets are selected for inference, e.g., based on proximity to the manipulator's base.

Things left to explore in future work are the introduction of obstacles such as rocks and tree stumps in the scenes, and simulation-to-real transfer using more realistic renders.

REFERENCES

- [1] D. Morrison, P. Corke, and J. Leitner, "Learning robust, real-time, reactive robotic grasping," *The International journal of robotics research*, vol. 39, no. 2-3, pp. 183–201, 2020.
- [2] S. Kumra, S. Joshi, and F. Sahin, "Antipodal robotic grasping using generative residual convolutional neural network," in *2020 IEEE/RSJ International Conference on Intelligent Robots and Systems (IROS)*. IEEE, 2020, pp. 9626–9633.
- [3] G. Zuo, J. Tong, H. Liu, W. Chen, and J. Li, "Graph-based visual manipulation relationship reasoning network for robotic grasping," *Frontiers in Neurorobotics*, vol. 15, 2021. [Online]. Available: <https://www.frontiersin.org/articles/10.3389/fnbot.2021.719731>
- [4] S. Ainetter and F. Fraundorfer, "End-to-end trainable deep neural network for robotic grasp detection and semantic segmentation from rgb," in *2021 IEEE International Conference on Robotics and Automation (ICRA)*. IEEE, 2021, pp. 13 452–13 458.
- [5] S. Wang, Z. Zhou, and Z. Kan, "When transformer meets robotic grasping: Exploits context for efficient grasp detection," *IEEE Robotics and Automation Letters*, vol. 7, no. 3, pp. 8170–8177, 2022.
- [6] Y. Jiang, S. Moseson, and A. Saxena, "Efficient grasping from RGBD images: Learning using a new rectangle representation," in *2011 IEEE International Conference on Robotics and Automation*, 2011, pp. 3304–3311.
- [7] A. Depierre, E. Dellandréa, and L. Chen, "Jacquard: A large scale dataset for robotic grasp detection," in *2018 IEEE/RSJ International Conference on Intelligent Robots and Systems (IROS)*, 2018, pp. 3511–3516.
- [8] G. Chalvatzaki, N. Gkanatsios, P. Maragos, and J. Peters, "Orientation attentive robotic grasp synthesis with augmented grasp map representation," 2021.
- [9] J. Andersson, K. Bodin, D. Lindmark, M. Servin, and E. Wallin, "Reinforcement learning control of a forestry crane manipulator," in *2021 IEEE/RSJ International Conference on Intelligent Robots and Systems (IROS)*, 2021, pp. 2121–2126.
- [10] E. Wallin, V. Wiberg, and M. Servin, "Multi-log grasping using reinforcement learning and virtual visual servoing," *Robotics*, vol. 13, no. 1, 2024. [Online]. Available: <https://www.mdpi.com/2218-6581/13/1/3>
- [11] P. La Hera, O. Mendoza-Trejo, O. Lindroos, H. Lideskog, T. Lindbäck, S. Latif, S. Li, and M. Karlberg, "Exploring the feasibility of autonomous forestry operations: Results from the first experimental unmanned machine," *Journal of Field Robotics*, vol. n/a, no. n/a, 2024. [Online]. Available: <https://onlinelibrary.wiley.com/doi/abs/10.1002/rob.22300>
- [12] E. Ayoub, P. Levesque, and I. Sharf, "Grasp planning with cnn for log-loading forestry machine," in *2023 IEEE International Conference on Robotics and Automation (ICRA)*, 2023, pp. 11 802–11 808.
- [13] J.-M. Fortin, O. Gamache, V. Grondin, F. Pomerleau, and P. Giguère, "Instance segmentation for autonomous log grasping in forestry operations," in *2022 IEEE/RSJ International Conference on Intelligent Robots and Systems (IROS)*, 2022, pp. 6064–6071.
- [14] A. Kirillov, E. Mintun, N. Ravi, H. Mao, C. Rolland, L. Gustafson, T. Xiao, S. Whitehead, A. C. Berg, W.-Y. Lo, P. Dollár, and R. Girshick, "Segment anything," 2023.
- [15] K. Hara, R. Vemulapalli, and R. Chellappa, "Designing deep convolutional neural networks for continuous object orientation estimation," 2017.
- [16] O. Ronneberger, P. Fischer, and T. Brox, "U-net: Convolutional networks for biomedical image segmentation," 2015.
- [17] Algoryx Simulations, "AGX Dynamics," Aug. 2021. [Online]. Available: <https://www.algoryx.se/products/agx-dynamics/>
- [18] K. Perlin, "An image synthesizer," in *Proceedings of the 12th Annual Conference on Computer Graphics and Interactive Techniques*, ser. SIGGRAPH '85. New York, NY, USA: Association for Computing Machinery, 1985, p. 287–296. [Online]. Available: <https://doi.org/10.1145/325334.325247>
- [19] Cranab AB, "Cranab CR HD Product sheet," Jun. 2023. [Online]. Available: <https://www.cranab.com/products/grapples-and-grapple-saws/cr-hd-grapples>
- [20] B. O. Community, *Blender - a 3D modelling and rendering package*, Blender Foundation, Stichting Blender Foundation, Amsterdam, 2018. [Online]. Available: <http://www.blender.org>